inorganics

MDPI

Article

New Aspects of Ruthenium-Mediated Polyhedral Contraction of Monocarbollides

Dmitry A. Loginov [1,2], Fedor M. Dolgushin [3], Vitalii E. Konoplev [4,*] and Maxim V. Tachaev [5]

1 A.N. Nesmeyanov Institute of Organoelement Compounds, Russian Academy of Sciences, 28, Vavilova St., 119991 Moscow, Russia
2 Higher Engineering School "New Materials and Technologies", Plekhanov Russian University of Economics, 36, Stremyanny per., 117997 Moscow, Russia
3 Kurnakov Institute of General and Inorganic Chemistry, Russian Academy of Sciences, 31, Leninsky Prosp., 119991 Moscow, Russia
4 Department of Materials Science and Engineering Technology, Institute of Mechanical and Power Engineering Named after V.P. Goryachkin, Russian State Agrarian University-Moscow Timiryazev Agricultural Academy, 49, Timiryazevskaya St., 127550 Moscow, Russia
5 Department of Inorganic Chemistry, Faculty of Science, Peoples Friendship University of Russia (RUDN University), 6, Miklukho-Maklaya St., 117198 Moscow, Russia
* Correspondence: konoplev@rgau-msha.ru

Abstract: It has been shown that the interaction of tris(triphenylphosphine)ruthenium dichloride $RuCl_2(PPh_3)_3$ (**1**) with 10-vertex monocarborane [6-Ph-*nido*-6-$CB_9H_{11}]^-[Et_4N]^+$ (**2**) under mild thermolysis conditions is not selective due to the undesired coordination of ruthenium to a phenyl substituent in the carborane and phosphine ligands, giving the series of new classical and non-classical metallacarborane complexes. In contrast, the reaction of **1** and monocarborane [*arachno*-6-$CB_9H_{14}]^-[Et_4N]^+$ (**3**) proceeds more selectively with the formation of the only one product, a *isocloso*-structured metallacarborane. The structures of two ruthenacarboranes were resolved by X-ray diffraction.

Keywords: ruthenium complexes; *isocloso*-metallacarborane; non-conventional clusters; organoboron compounds; NMR; structure

check for updates

Citation: Loginov, D.A.; Dolgushin, F.M.; Konoplev, V.E.; Tachaev, M.V. New Aspects of Ruthenium-Mediated Polyhedral Contraction of Monocarbollides. *Inorganics* **2022**, *10*, 158. https://doi.org/10.3390/inorganics10100158

Academic Editor: Rainer Winter

Received: 30 August 2022
Accepted: 23 September 2022
Published: 28 September 2022

1. Introduction

Metallacarboranes are of particular interest due to their unique structures in which the metal atom is covalently bonded to the carborane polyhedron [1–3]. In the last decade, they have found a wide range of applications in catalysis [4,5]. In particular, the introduction of substituents into the carborane ligand allows to tune on the electronic, steric, and enantioselective properties of the catalyst. Thus, metallacarboranes showed good catalytic efficiency for amination of carbonyl compounds [6], radical polymerization of methyl methacrylate [7–10], oxidative coupling of benzoic acids and arenes with internal alkynes [11–14], carbene transfer reactions [15], as well as hydrogenation, isomerization, and metathesis of olefins [16–18]. Very recently, Romero and Teixidor with co-workers demonstrated the use of the cobalt bis(dicarbollide) anion and its derivatives as photocatalysts in various organic transformations [19–21].

Another way to modify electronic and steric parameters of metallacarboranes are the polyhedral contraction reactions, which occur with the removal of BH vertices [22–24]. However, many such reactions are not clean and selective, which reduces their use in synthesis. In continuation of our studies on the polyhedral contraction [25,26], in this work, we studied reactions of the electron-deficient complex $RuCl_2(PPh_3)_3$ (**1**) with 10-vertex monocarboranes [6-Ph-*nido*-6-$CB_9H_{11}]^-[Et_4N]^+$ (**2**) and [*arachno*-6-$CB_9H_{14}]^-[Et_4N]^+$ (**3**) to compare their outcome and selectivity. It turned out that the presence of phenyl substituent

in **2** significantly complicates the polyhedral contraction due to undesirable coordination of this substituent, while carborane **3** reacts smoothly, giving only one ruthenacarborane.

2. Results and Discussion

We found that refluxing of carborane **2** and ruthenium complex **1** in MeOH gives new 10-vertex clusters **4a**,**b** and **5a**,**b**, zwitterionic ruthenium arene complex **6**, as well as 8-vertex ruthenacarboranes **7a**,**b** with a total yield of ~25% (Scheme 1). We have previously shown that a similar reaction of **2** with the osmium complex $OsCl_2(PPh_3)_3$ is more selective and gives the *isocloso*-{$OsCB_8$} cluster as the only stable product [25].

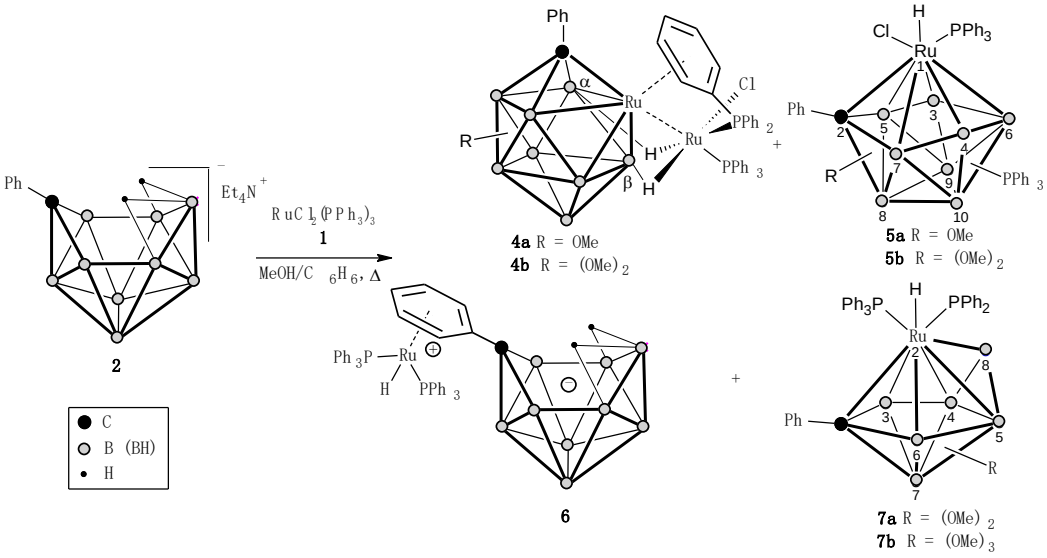

Scheme 1. Reaction of $RuCl_2(PPh_3)_3$ (**1**) with tetraethylammonium 6-phenyl-*nido*-6-carbadecaborate (**2**).

According to the X-ray diffraction data (Figure 1), diruthenacarborane 1-Ph-2-[5,9-*exo*-$RuClPPh_3(\mu,\eta^6\text{-}C_6H_5PPh_2)$]-5,9-$(\mu\text{-}H)_2$-*closo*-2,1-$RuCB_8H_5(OMe)$ (**4a**) has the geometry of a bicapped tetragonal antiprism and belongs to the classical 10-vertex clusters (22 skeletal electrons). The Ru(1) atom coordinates one chloride and two triphenylphosphine ligands, forming an *exo*-$RuClPPh_3(PPh_2\text{-}\mu,\eta^6\text{-}C_6H_5)]^+$ fragment, which is bonded to the carborane frame via two B-H···Ru bonds involving boron atoms located in the α- and β-positions relative to the carbon atom. Notably, the formation of **4a** is accompanied by the incorporation of methoxy to the 6-positioned boron atom and the loss of one boron vertex. Probably, the methoxylation of carborane cage is the first step of the polyhedral contraction, and methanol plays a key role in this fascinating process. For example, Stone with co-workers showed that the reaction of **2** with $[ReBr(thf)_2(CO)_3]$ in non-alcoholic solvent (THF) leads to 11-vertex {$ReCB_9$} species without loss of BH vertexes [27]. Moreover, we recently found that polyhedral contraction can occur not only simultaneously upon coordination with a metal atom, but also upon simple boiling of a preliminarily prepared metallacarborane in methanol [26].

A similar structure was proposed for 1-Ph-2-[5,9-*exo*-$RuClPPh_3(\mu,\eta^6\text{-}C_6H_5PPh_2)$]-5,9-$(\mu\text{-}H)_2$-*closo*-2,1-$RuCB_8H_4(OMe)_2$ (**4b**), which has two methoxy-substituents in the carborane ligand in contrast to **4a**. Thus, the ^1H NMR spectra of **4a**,**b** contain signals of MeO groups with δ 3.88 ppm (**4a**) and 3.46, 3.86 ppm (**4b**) with a relative intensity of 3H. Unfortunately, the exact position of the substituents in **4b** has not been determined, since we were not able to obtain single crystals suitable for X-ray crystallography.

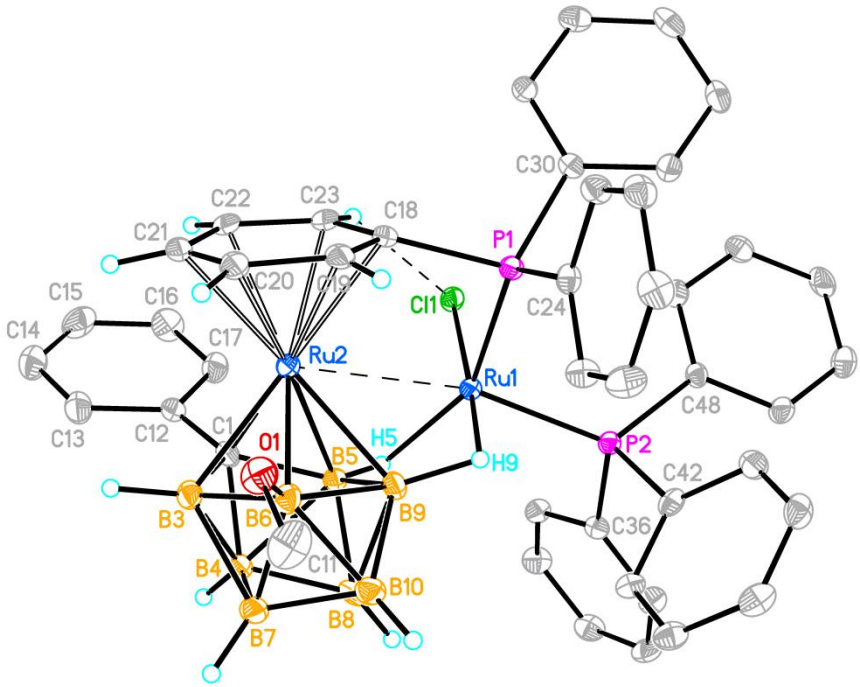

Figure 1. Molecular structure of the complex **4a** (only the hydrogen atoms of the carborane and η^6-phenyl moieties are shown; thermal ellipsoids are drawn at the 30% probability level). Selected interatomic distances (Å) for two independent molecules A/B are: Ru(1)···Ru(2) 2.9261(6)/2.9101(6), Ru(1)-Cl(1) 2.418(1)/2.430(1), Ru(1)-P(1) 2.224(1)/2.241(1), Ru(1)-P(2) 2.273(1)/2.279(1), Ru(1) . . . B(9) 2.234(4)/2.242(4), Ru(1) . . . B(5) 2.372(4)/2.356(4), Ru(1)-H(5) 2.00(3)/2.04(3), Ru(1)-H(9) 1.67(4)/1.56(4), Ru(2)-C(1) 2.083(3)/2.101(3), Ru(2)-B(3,5,6,9) 2.231(4)-2.306(4), Ru(2)-C(18-23) 2.221(3)-2.303(4), P(1)-C(18) 1.844(4)/1.837(4), C(1)-C(12) 1.484(5)/1.498(5).

The ^{1}H NMR spectra of **4a**,**b** also contain a set of broad high-field signals corresponding to the bridging protons of B-H···Ru groups (δ −3.34, −16.34 and −3.30, −15.83 ppm for **4a** and **4b**, respectively). It can be seen that the chemical shifts in the bridging H atoms differ greatly. A similar phenomenon was previously observed in "three-bridged" *exonido*-osmacarboranes *exonido*-5,6,10-[Cl(Ph$_3$P)$_2$Os]-5,6,10-(μ-H)$_3$-10-H-7-R-8-R^1-7,8-C$_2$B$_9$H$_6$ (R, R^1 = H, Alk) [28], where it was rigorously proven that the downfield B-H···Os bond signal corresponds to the bridging hydrogen atom that occupies the *trans*-position relative to the Os-Cl bond in the octahedral environment of the metal atom. By analogy, the signals B-H···Ru(1) with δ −16.34 and −15.83 ppm in ^{1}H NMR spectra of **4a,b** were attributed to H(9) atoms, and the signals with δ −3.34 and −3.30 ppm were attributed to H(5).

In addition, the ^{1}H NMR spectra of both complexes contain signals characteristic of a coordinated arene ligand: a set of four well-resolved multiplets in the range δ 6.0−4.0 ppm. Each of these signals corresponds to one proton; the fifth signal overlaps with proton signals of uncoordinated phenyl rings. The downfield shift in the signal of one of the hydrogen atoms of the bridging μ,η^6-phenyl ligand can be explained by its participation in the intramolecular Ph-*o*-H···Cl hydrogen bond. According to X-ray diffraction data for complex **4a**, the distance between H(23A) and the Cl atom (2.48 Å) is shorter than the sum of the corresponding Van der Waal radii (2.86 Å [29]) and the C-H···Cl angle is 141.4° (average values are given for two independent molecules). Such μ,η^6-coordination of triphenylphosphine ligands is known for a number of complexes [30]. Among them, several crystallographically studied clusters belonging to polyhedral boron-containing complexes are described: PMe$_2$Ph-μ-η^6(Ru)-η^1(Pt)-(C$_6$H$_5$PPh$_2$)-*closo*-PtRuB$_9$H$_9$ [31] and μ,η^6-C$_6$H$_5$PPh$_2$)]-7,11-(μ-H)$_2$-*closo*-2,1-RuCB$_{10}$H$_8$R (R = H, 6-OMe, 3-OMe) [32], in which the phosphine ligand on the one metal acts as an η^6-coordinated ligand with respect to another metal atom.

Other products of the reaction discussed are mononuclear 10-vertex *isocloso* complexes: 1,3-$(PPh_3)_2$-1-H-1-Cl-2-Ph-4-OMe-*isocloso*-1,2-$RuCB_8H_6$ (**5a**) and 1-PPh_3-1-H-1-Cl-2-Ph-4-OMe-*isocloso*-1,2-$RuCB_8H_5(OMe)(PPh_3)$ (**5b**), which belong to electron-deficient 2*n* clusters (20 skeletal electrons). We used label "*isocloso*" for these compounds to emphasize their non-conventional structure, which is quite distinct from the cluster geometry of classically structured closo 10-vertex metallacarbaboranes [33]. Similar to **4a**,**b**, the formation of **5a**,**b** is also accompanied by the deboronation of the carborane framework and the methoxylation process, which leads to a mixture of mono- and dimethoxy-substituted derivatives. It should be noted that monomethoxy substituted compound **5a** is indefinitly stable and does not transform into **5b** upon boiling in methanol.

According to X-ray diffraction analysis (Figure 2), complex **5a** has the geometry of a 10-vertex polyhedron with the $\{CB_8\}$ carborane ligand substituted with the MeO group and triphenylphosphine at the boron atoms. The ruthenium atom coordinates the six-membered $\{CB_5\}$ open face of carborane in the *hexahapta* chair conformation. The metallacarborane cage has idealized C_{3v} symmetry with the ruthenium atom in the axial position. In the molecule, there are three short distances from the Ru(1) atom to the C(2), B(3), and B(4) atoms with a cluster coordination number of 4 [2.188(14), 2.063(13), 2.090(14) Å) and three longer distances to B(5), B(6), and B(7) atoms with a coordination number of 5 [2.448(14), 2.364(11), 2.514(14) Å].

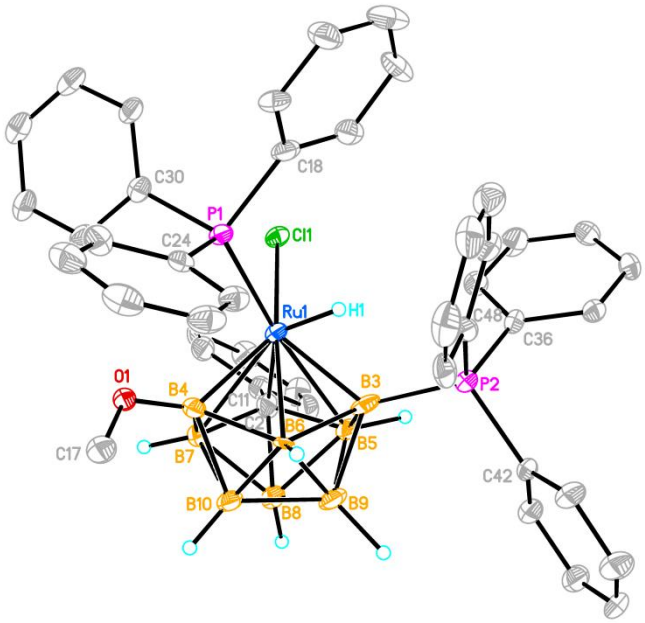

Figure 2. Molecular structure of the complex **5a** (only the hydrogen atoms of the hydride ligand and carborane moiety are shown; thermal ellipsoids are drawn at the 30% probability level). Selected interatomic distances (Å) are: Ru(1)-Cl(1) 2.411(3), Ru(1)-P(1) 2.351(3), Ru(1)-H(1) 1.34, Ru(1)-C(2) 2.181(11), Ru(1)-B(7) 2.516(12), Ru(1)-B(5) 2.449(11), Ru(1)-B(4) 2.095(11), Ru(1)-B(3) 2.072(11), Ru(1)-B(6) 2.364(9), P(2)-B(3) 1.889(13), C(2)-C(11) 1.478(15).

The ^{11}B NMR spectra of complexes **5a** and **5b** contain three groups of signals in the range δ −30–+83 ppm. The signals of the first group are in a low field (δ from +64 to +83 ppm) and, in accordance with [34], are assigned to B(3) and B(4) atoms, which have a low coordination number equal to 4. Since one of the signals is present as a singlet, it can be concluded that the boron atom [B(3) or B(4)] corresponding to this signal has a MeO substituent. The evidence that in complexes **5a** and **5b** one of the PPh_3 groups is also bound to the boron atom is the presence of doublet splitting with $^1J(P,B)$ = 160 and 138 Hz, respectively, in one of the signals in the $^{11}B/^{11}B\{^1H\}$ NMR spectra of these compounds. Despite the presence of two different PPh_3 groups in complexes **5a** and **5b** (at the metal atom and in the carborane ligand), in the ^1H NMR spectra, the signal of the terminal

hydride appears as a broadened doublet with a spin–spin coupling constant ^2J(P,H) = 63 and 43 Hz, respectively. However, in the ^{1}H{^{11}B} NMR spectrum of complex **5a** (with complete decoupling from ^{11}B), the hydride signal already has the form of a doublet of doublets, and the long-range spin–spin coupling constant ^3J(P,H) = 16 Hz can be observed experimentally. The position of the triphenylphosphine substituent as well as the second methoxy group in **5b** is not defined.

The zwitterionic mononuclear complex 6-[η^6-$C_6H_5RuH(PPh_3)_2$-*nido*-6-CB_9H_{11} (**6**) was also isolated in the reaction in low yield. The structure of complex **6** was determined from the ^{1}H and ^{31}P{^{1}H} NMR spectra. According to the C_s symmetry, the ^{11}B NMR spectrum of complex **6** contains a set of six signals with a relative intensity of 2:1:2:2:1:1. In the ^{31}P{^{1}H} NMR spectrum, there is one singlet signal from two equivalent PPh_3 groups with δ 53.8 ppm. In the ^{1}H NMR spectrum, a high-field broad signal was found corresponding to two bridging (B-H-B) hydrogen atoms of carborane (δ −3.17 ppm) and a terminal hydride triplet signal [δ −9.95 ppm, J(P,H) = 38 Hz].

The ruthenium atom η^6-coordinates the phenyl group of the carborane, as well as one hydride and two triphenylphosphine ligands. At the same time, the carborane ligand in **6** retains two B–H–B bridging hydrogen atoms in the same position as in the starting carborane **2**, i.e., it formally has a negative charge. Taking into account that the ruthenium atom coordinates only one hydride ligand, it should be concluded that complex **6** is zwitterionic, and the metal atom has a formal oxidation state of +2. A similar example of zwitterionic metallacarboranes, 6-[η^6-$C_6H_5RuH(PPh_3)_2$-*nido*-7,9-$C_2B_9H_{11}$, is described in the literature [35].

Among the reaction products, another group of metallacarboranes with an extraordinary structure was found, which belongs to rare 8-vertex capped *closo*-clusters with a boron vertex built over a triangular face. Two compounds of this type were isolated by column chromatography: capped *closo*-l-Ph-2,2-(PPh_3)2-2-H-3,8-$(OMe)_2$-6-R-2,1-$RuCB_6H_3$ [R = H (**7a**), R = OMe (**7b**)], which are products of a deeper degradation (the loss of two boron vertices) of the initial carborane **2**.

Structure of compounds **7a,b** was confirmed using the ^{1}H, ^{31}P{^{1}H}, ^{11}B/^{11}B{^{1}H} NMR and mass spectroscopic data by analogy with the carbon-unsubstituted analogue capped *closo*-2,2-$(PPh_3)_2$-2-H-3,6,8-$(OMe)_3$-2,1-$RuCB_6H_4$ (Table 1), whose structure was unambiguously confirmed previously by X-ray diffraction [36].

Table 1. Selected NMR Data for **7a,b** and capped *closo*-2,2-$(PPh_3)_2$-2-H-3,6,8-$(OMe)_3$-2,1-$RuCB_6H_4$.

NMR		7a	7b	$(PPh_3)_2HRuCB_6H_4(OMe)_3$ [36]
^{1}H	OMe	4.24 s (3H); 2.96 s (3H)	4.27 s (3H); 2.80 s (6H)	4.17 s (3H); 3.05 s (6H)
	H_{Ru}	−9.84 br t (1H), ^2J(H,P) = 24 Hz	−10.43 br t (1H), ^2J (H,P) = 24 Hz	−9.02 br t (1H), ^2J(H,P) = 20.7 Hz
^{31}P{^{1}H}	PPh_3	46.2 d (1P), ^2J = 10 Hz; 46.0 d (1P), ^2J = 10 Hz	48.3 s (2P)	49.4 s (2P)
^{11}B{^{1}H}	B-8	67.5 s (1B)	70.1 s (1B)	68.9 s (1B)
	B-3,6	33.7 s (1B); 24.1 s (1B)	32.8 s (2B)	33.7 s (2B)
	B-7	14.0 s (1B)	14.1 s (1B)	12.8 s (1B)
	B-4,5	−26.3 (1B); −30.1 (1B)	−32.4 s (2B)	−31.8 s (2B)

In the ^{1}H NMR spectrum of complex **7b**, two of the three MeO groups appear as a single signal (δ 2.8 ppm) with an intensity of 6H, which indicates their equivalence and, therefore, the location at the B(3) and B(6) (both are in the α-position relative to the carbon atom). Taking into account the preservation of symmetry in this complex, the third MeO-group should be bound to the B(8) atom, which is located symmetrically over the Ru(2)-B(4)-B(5) face. In the ^{1}H NMR spectrum, the signal of the terminal hydride has the

form of a broadened triplet, while in the $^{31}P\{^1H\}$ NMR spectrum, only one singlet signal (δ 48.3 ppm) from two equivalent PPh_3 ligands bound to the metal atom is observed. In the $^{11}B\{^1H\}$ NMR spectrum of **7b**, in accordance with the C_s symmetry, a set of four signals with a relative intensity of 1:2:1:2 is observed. Extremely weak field signal with δ 70.1 ppm confirms the presence of a coordinatively unsaturated B(8) atom in the complex.

Complex **7a** with two MeO groups has C_1 symmetry. Therefore, in the ^{11}B NMR spectrum, six signals appear, each with an intensity of 1B. Two of these signals are singlets, which indicates two MeO substituents associated with the carborane ligand. Here, as in spectrum of **7b**, one signal from the B(8) atom appears in a much weaker field than the others (the assignment of some of them was performed by analogy with complex **7b**). The $^{31}P\{^1H\}$ NMR spectrum of **7a** contains two doublet signals with δ 46.2 and 46.0 ppm with ^2J(P,P) = 10 Hz. Accordingly, in the ^1H NMR spectrum, the hydride signal appears as a broadened triplet with ^2J(P,H) = 24 Hz.

In contrast to the previous reaction, $RuCl_2(PPh_3)_3$ under similar conditions selectively reacts with monocarbon carborane [*arachno*-6-$CB_9H_{14}]^-[Et_4N]^+$ (**3**), forming 10-vertex ruthenacarborane 1,1-$(PPh_3)_2$-1-H-3-OMe-*isocloso*-1,2-$RuCB_8H_7$ (**8**) as the only stable product in 26% yield (Scheme 2). The higher selectivity in this case can be explained by the absence of phenyl substituent in **3**, which significantly complicates the reactions due to the strong coordination affinity of ruthenium to arene ligands [37].

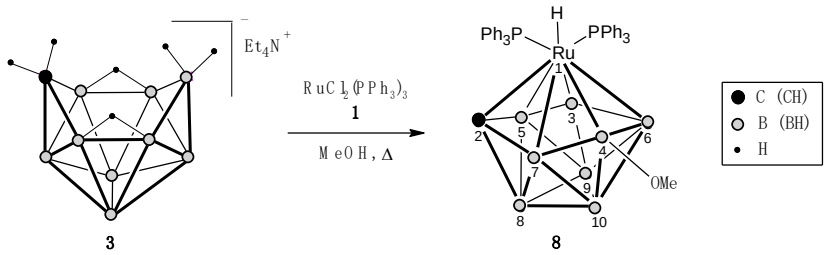

Scheme 2. Reaction of $RuCl_2(PPh_3)_3$ (**1**) with tetraethylammonium *arachno*-6-carbadecaborate (**3**).

The structure of **8** was established on the basis of the ^1H, $^{31}P\{^1H\}$, and $^{11}B/^{11}B\{^1H\}$ NMR spectra. The ^1H NMR spectrum contains a signal of the hydrogen atom of the CH group of the carborane ligand (δ 7.83 ppm), which is a doublet with ^2J(P,H) = 10 Hz, and one singlet signal of the MeO group (δ 4.03 ppm). The hydride signal with δ −5.30 ppm appears as a broadened doublet of doublets with $^2J(P^a,H)$ = 22 Hz and $^2J(P^b,H)$ = 46 Hz. In the $^{31}P\{^1H\}$ NMR spectrum, one of the two signals of the phosphorus atoms of triphenylphosphine ligands is a broadened singlet (δ 49.2 ppm), and the second is a doublet (δ 35.9 ppm) with $^2J_{AB}$ = 15 Hz, probably due to the *trans*-location of the first ligand relative to one of the boron atoms of the carborane fragment. In the ^{11}B NMR spectra of complex **8**, as well as in the spectra of ruthenacarboranes **5a,b**, there is a broad singlet signal (δ 83.1 ppm) with doubled intensity, which we attributed to two coordinatively unsaturated atoms B(3) and B(4). Since the remaining signals in the spectrum have the form of doublets with their usual spin–spin coupling constant ^1J(B,H) in the range of 130–145 Hz, it can be concluded that the MeO group is located precisely at one of these boron atoms, B(3) or B(4) (the positions are equivalent).

3. Materials and Methods

3.1. General Procedures

The reaction described above was carried out using standard Schlenk equipment under an atmosphere of dry argon. All solvents, including those used for column chromatography as eluents, were dried under appropriate drying agents and distilled under argon prior to use. The reactions products were isolated by column chromatography and purified by crystallization in air. Chromatography was performed on silica gel (Merck, 70–230 mesh). The NMR spectra were obtained with a Bruker AMX-400 spectrometer (^1H, 400.13 MHz; ^{31}P, 161.98 MHz; ^{11}B, 128.33 MHz) using TMS as an internal reference and 85% H_3PO_4 and

$BF_3 \cdot Et_2O$ as the external references, respectively. Microanalyses were performed at the Analytical Laboratory of the Institute of Organoelement Compounds of the RAS. The starting material, tris(triphenylphosphine)ruthenium dichloride (**1**) was prepared by methods published elsewhere [38]. Tetraethylammonium 6-phenyl-*nido*-6-carbadecaborate (**2**) and tetraethylammonium *arachno*-6-carbadecaborate (**3**) were obtained from the laboratory of Prof. Kennedy J.D. (University of Leeds, Leeds, UK).

*3.2. Reaction of $RuCl_2(PPh_3)_3$ (**1**) with Tetraethylammonium 6-Phenyl-Nido-6-Carbadecaborate (**2**)*

A solution of complex **1** (1 g, 1.04 mmol) in 50 mL of benzene was added dropwise over 2 h to a stirred solution of *nido*-carborane **2** (0.38 g, 1.16 mmol) in 50 mL of anhydrous methanol under argon at low boiling. The use of toluene as a co-solvent instead of benzene leads to a significant decrease in the yield of products. The solution was refluxed with stirring for another 3 h, while the color of the reaction mixture changed from brown to dark red. After cooling the reaction mixture and removing the solvent, the solid residue was placed on a silica gel column 63–210 μm, eluting with CH_2Cl_2. The first light yellow fraction containing PPh_3, **6**, and **7a**,**b**, and the next two red fractions, **4a**, **5a** and **4b**, **5b**. The mixture of products from the light yellow fraction was separated again on a column of silica gel in benzene, washing off, successively, **7a**, **7b**, and **6**. The products from the two red fractions were also chromatographed on a column of silica gel using CH_2C1_2/*n*-hexane (2:1) as the eluent; from the first red fraction, an orange substance **5a** and a red substance **4a** were obtained; from the second red fraction, an orange product **5b** and a red product **4b**. The complexes were finally purified by recrystallization from a CH_2C1_2/*n*-hexane solvent mixture.

*1-Ph-2-[5,9-exo-RuClPPh$_3$(μ,η^6-C$_6$H$_5$PPh$_2$)]-5,9-(μ-H)$_2$-closo-2,1-RuCB$_8$H$_5$(OMe) (**4a**).* Yield 64 mg, 6%. IR, ν/cm^{-1}: 2546 (B-H). ^{1}H NMR (400.13 MHz, CD_2Cl_2): δ 7.83, 7.60–7.18, 6.84 m, 30H + 1H (H_{Ph}); 5.91 t, 1H, *J* = 6 Hz (η-Ph); 5.53 t, 1H, *J* = 6 Hz (η-Ph); 5.05 t, 1H, *J* = 6 Hz (η-Ph); 4.16 t, 1H, *J* = 6 Hz (η-Ph); 3.88 s, 3H (OMe); −3.34 br m, 1H (H-5); −16.34 br m, 1H (H-9). ^{31}P{^{1}H} NMR (161.98 MHz, CD_2Cl_2): δ 64.1 d, 1P, $^2J_{AB}$ = 32 Hz; 59.2 d, 1P, $^2J_{AB}$ = 32 Hz. ^{11}B NMR (128.33 MHz, CD_2Cl_2): δ 42.5 s, 1B; 16.6 d, 1B, ^1J(B,H) = 137 Hz; 10.9 d, 2B, ^1J(B,H) = 145 Hz; 8.6 d, 1B, ^1J(B,H) = 137 Hz; −6.5 d, 1B, ^1J(B,H) = 143 Hz; −20.2 d, 2B, ^1J(B,H) = 131 Hz. For $C_{44}H_{45}B_8ClOP_2Ru_2$ (975.86) calculated (%): C, 54.15; H, 4.65; B, 8.86; P, 6.35. Found (%): C, 54.05; H, 4.52; B, 8.97; P, 6.28.

*1-Ph-2-[5,9-exo-RuClPPh$_3$(μ,η^6-C$_6$H$_5$PPh$_2$)]-5,9-(μ-H)$_2$-closo-2,1-RuCB$_8$H$_4$(OMe)$_2$ (**4b**).* Yield 54 mg, 5%. IR, ν/cm^{-1}: 2541 (B-H). ^{1}H NMR (400.13 MHz, CD_2Cl_2): δ 7.83–7.15, 6.94 m, 30H + 1H (H_{Ph}); 5.76 t, 1H, *J* = 6 Hz (η-Ph); 5.44 t, 1H, *J* = 6 Hz (η-Ph); 4.88 t, 1H, *J* = 6 Hz (η-Ph); 3.98 t, 1H, *J* = 6 Hz (η-Ph); 3.86 s, 3H (OMe); 3.46 s, 3H (OMe); −3.30 br m, 1H (H-5); −15.83 br m, 1H (H-9). ^{31}P{^{1}H} NMR (161.98 MHz, CD_2Cl_2): δ 63.1 d, 1P, $^2J_{AB}$ = 32 Hz; 58.3 d, 1P, $^2J_{AB}$ = 32 Hz. ^{11}B NMR (128.33 MHz, CD_2Cl_2): δ 38.0 br s, 1B; 27.5 br s, 1B; 4.8 br s, 2B; −12.4 br s, 1B; −22.6 br s, 2B; −31.4 br s, 1B. For $C_{45}H_{47}B_8ClO_2P_2Ru_2$ (1005.88) calculated (%): C, 53.73; H, 4.71; B, 8.60; P, 6.16. Found (%): C, 53.54; H, 4.69; B, 8.71; P, 6.21.

*1,3-(PPh$_3$)$_2$-1-H-1-Cl-2-Ph-4-OMe-isocloso-1,2-RuCB$_8$H$_6$ (**5a**).* Yield 35 mg, 4%. IR, ν/cm^{-1}: 2531 (B-H); 1989 (Ru-H). ^{1}H{^{11}B} NMR (400.13 MHz, CD_2Cl_2): δ 7.92–7.06 m, 6.03 t, 28H + 2H (H_{Ph}); 3.64 br s, 1H (BH); 3.44 br s, 1H (BH); 3.16 br s, 1H (BH); 2.99 s, 3H (OMe); 2.85 br s, 1H (BH); 2.69 br s, 1H (BH); 0.00 br s, 1H (BH); −5.44 dd, 1H, ^2J(P,H) = 16 Hz, ^2J(P,H) = 63 Hz (H_{Ru}). ^{31}P{^{1}H} NMR (161.98 MHz, CD_2Cl_2): δ 50.1 s, 1P (Ru-PPh_3); 8.4 q, 1P, ^1J(P,B) = 160 Hz (B-PPh_3). ^{11}B NMR (128.33 MHz, CD_2Cl_2): δ 82.9 s, 1B (B-4); 64.5 d, 1B, ^1J(B,P) = 160 Hz (B-3); 14.1 d, 1B, ^1J(B,H) = 141 Hz (B-9); 12.5 d, 1B, ^1J(B,H) = 137 Hz (B-10); 1.7 d, 1B, ^1J(B,H) = 146 Hz (B-8); −6.9 d, 1B, ^1J(B,H) = 118 Hz (B-7); −9.8 d, 1B, ^1J(B,H) = 128 Hz (B-5); −21.8 d, 1B, ^1J(B,H) = 131 Hz (B-6). ^{13}C{^{1}H} NMR (100.51 MHz, CD_2Cl_2): δ 169.8 br s (C_{carb}); 147.5, 136.0−126.6, 123.5, 122.9 (C_{Ph}); 57.8 s (OMe). For $C_{44}H_{45}B_8ClOP_2Ru$ (874.79) calculated (%): C, 60.41; H, 5.18; B, 9.89; P, 7.08. Found (%): C, 60.36; H, 5.22; B, 10.02; P, 6.98.

1-PPh$_3$-1-H-1-Cl-2-Ph-4-OMe-isocloso-1,2-RuCB$_8$H$_5$(OMe)(PPh$_3$) (**5b**). Yield 24 mg, 3%. IR, ν/cm^{-1}: 2536 (B-H); 1999 (Ru-H). ^{1}H NMR (400.13 MHz, CD_2Cl_2): δ 7.53-7.23 m, 35H (H_{Ph}); 4.15 s, 3H (OMe); 3.71 s, 3H (OMe); −3.11 br d, 1H, ^2J(H,P) = 43 Hz (H_{Ru}). ^{31}P{^{1}H} NMR (161.98 MHz, CD_2Cl_2): δ 45.9 s, 1P (Ru-P); 5.3 br q, 1P (B-P). ^{11}B NMR (128.33 MHz, CD_2Cl_2): δ 79.4 s, 1B (B-4); 73.5 d, 1B, ^1J(B,H) = 96 Hz (B-3); 16.6 d, 1B, ^1J(B,H) = 122 Hz [B-8 (9 or 10)]; 13.4 s, 1B [B-5 (6 or 7)]; 8.41 d, 2B, ^1J(B,H) = 112 Hz [B-9,10 (8,10 or 8,9)]; −26.7 d, 1B, ^1J(B,H) = 151 Hz [B-6 (7 or 5)]; −29.8 d, 1B, ^1J(B,P) = 138 Hz [B-7 (5 or 6)]. For $C_{45}H_{47}B_8ClO_2P_2Ru$ (904.81) calculated (%): C, 59.73; H, 5.24; B, 9.56; P, 6.85. Found (%): C, 60.01; H, 5.21; B, 9.58; P, 6.76. *m/z* 904.2 [M]$^+$.

6-[(η^6-C$_6$H$_5$)RuH(PPh$_3$)$_2$]-nido-CB$_9$H$_{11}$ (**6**). Yield 14 mg, 2%. IR, ν/cm^{-1}: 2534 (B-H); 1985 (Ru-H). ^{1}H NMR (400.13 MHz, CD_2Cl_2): δ 7.34−7.16 m, 30H (PPh_3); 6.13 t, 1H, ^3J(H,H) = 5.5 Hz (H_{para}, η-Ph); 5.05 d, 2H, ^3J(H,H) = 6.5 Hz (H_{ortho}, η-Ph); 4.85 t, 2H, ^3J(H,H) = 6 Hz (H_{meta}, η-Ph); −3.17 br s, 2H (μ-H); −8.95 t, 1H, ^2J(H,P) = 38 Hz (H_{Ru}). ^{31}P{^{1}H} NMR (161.98 MHz, CD_2Cl_2): δ 53.8 s, 2P (PPh_3). ^{11}B NMR (128.33 MHz, CD_2Cl_2): δ 4.0 d, 2B, ^1J(B,H) = 142 Hz; 2.1 d, 1B, ^1J(B,H) = 80 Hz; −3.2 d, 2B, ^1J(B,H) = 141 Hz; −11.5 d, 2B, ^1J(B,H) = 115 Hz; −25.7 d, 1B, ^1J(B,H) = 158 Hz; −35.6 d, 1B, ^1J(B,H) = 143 Hz. For $C_{43}H_{37}B_9P_2Ru$ (824.15) calculated (%): C, 62.67; H, 5.75; B, 11.81; P, 7.52. Found (%): C, 62.61; H, 5.71; B, 11.92; P, 7.48. *m/z* 824.3 [M]$^+$.

Capped closo-1-Ph-2,2-(PPh$_3$)$_2$-2-H-3,8-(OMe)$_2$-2,1-RuCB$_6$H$_4$ (**7a**). Yield 24 mg, 3%. IR, ν/cm^{-1}: 2522 (B-H); 2050 (Ru-H). ^{1}H NMR (400.13 MHz, CD_2Cl_2): δ7.30−6.97 m, 35H (H_{Ph}); 4.24 s, 3H (OMe); 2.96 s, 3H (OMe); −9.84 br t, 1H, ^2J(H,P) = 24 Hz (H_{Ru}). ^{31}P{^{1}H} NMR (161.98 MHz, CD_2Cl_2): δ 46.2 d, 1P, $^2J_{AB}$ = 10 Hz; 46.0 d, 1P, $^2J_{AB}$ = 10 Hz. ^{11}B NMR (160.46 MHz, CD_2Cl_2): δ 67.5 s, 1B (B-8); 33.7 s, 1B (B-3); 24.1 br s, 1B [B-6 (7)]; 14.0 d, 1B, ^1J(B,H) = 147 Hz [B-7 (6)]; -26.3 d, 1B, ^1J(B,H) = 149 Hz [B-4 (5)]; −30.1 d, 1B, ^1J(B,H) = 147 Hz [B-5 (4)]. For $C_{45}H_{46}B_6O_2P_2Ru$ (846.73) calculated (%): C, 63.83; H, 5.48; B, 7.66; P, 7.32. Found (%): C, 63.75; H, 5.52; B, 7.51; P, 7.16. *m/z* 847.3 [M]$^+$.

Capped closo-1-Ph-2,2-(PPh$_3$)$_2$-2-H-3,6,8-(OMe)$_3$-2,1-RuCB$_6$H$_3$ (**7b**). Yield 10 mg, 1%. IR, ν/cm^{-1}: 2517 (B-H); 2043 (Ru-H). ^{1}H NMR (400.13 MHz, CD_2Cl_2): δ 7.24−6.96 m, 6.48 d, 35H (H_{Ph}); 4.27 s, 3H (OMe); 2.80 s, 6H (OMe); −10.43 br t, 1H, ^2J(H,P) = 24 Hz (H_{Ru}). ^{31}P{^{1}H} NMR (161.98 MHz, CD_2Cl_2): δ 48.3 s, 2P. ^{11}B{^{1}H} NMR (128.33 MHz, CD_2Cl_2): δ 70.1 s, 1B (B-8); 32.8 s, 2B (B-3,6); 14.1 s, 1B (B-7); −32.4 s, 2B (B-4,5). For $C_{46}H_{48}B_6O_3P_2Ru$ (876.76) calculated (%): C, 63.02; H, 5.52; B, 7.40; P, 7.07. Found (%): C, 63.38; H, 5.49; B, 7.48; P, 7.34. Found: *m/z* 876.4 [M]$^+$.

*3.3. Reaction of RuCl$_2$(PPh$_3$)$_3$ (**1**) with Tetraethylammonium Arachno-6-Carbadecaborate (**3**)*

Complex **1** (0.5 g, 0.52 mmol) was added to a stirred solution of *arachno*-carborane **3** (0.16 g, 0.63 mmol) in 15 mL of absolute methanol under argon. The mixture was refluxed with stirring for 14 h. Gradually, the precipitate turned from brown to yellow. The reaction mixture was cooled, and after removing the solvent, the resulting oily residue was chromatographed through a silica-gel column (63–210 μm) in a mixture of solvents CH_2Cl_2/*n*-hexane (2:1). After crystallization from a mixture of solvents CH_2Cl_2/*n*-hexane, yellow crystals of complex **8** were obtained.

1,1-(PPh$_3$)$_2$-1-H-3-OMe-isocloso-*1,2-RuCB$_8$H$_7$* (**8**). Yield 0.11 g, 26%. IR, ν/cm^{-1}: 2538 (B-H); 1990 (Ru-H). ^{1}H NMR (400.13 MHz, CD_2Cl_2): δ 7.83 br d, 1H, ^3J(H,P) = 10 Hz (CH_{carb}); 7.40−7.16 m, 30H (Ph); 4.03 s, 3H (OMe); −5.30 br dd, 1H, ^2J(P^a,H) = 22 Hz, ^2J(P^b,H) = 46 Hz (H_{Ru}). ^{31}P{^{1}H} NMR (161.98 MHz, CD_2Cl_2): δ 49.2 br s, 1P; 35.9 d, 1P, $^2J_{AB}$ = 15 Hz. ^{11}B NMR (128.33 MHz, CD_2Cl_2): δ 83.1 br s, 2B (B-3,4); 16.6 d, 1B, ^1J(B,H) = 137 Hz [B-8 (9 or 10)]; 10.9 d, 1B, ^1J(B,H) = 145 Hz [B-9 (10 or 8)]; 8.6 d, 1B, ^1J(B,H) = 137 Hz [B-10 (8 or 9)]; −6.5 d, 1B, ^1J(B,H) = 143 Hz [B-5 (6 or 7)]; −20.2 d, 2B, ^1J(B,H) = 131 Hz [B-6,7 (5,7 or 5,6)]. For $C_{38}H_{42}B_8OP_2Ru$ (764.25) calculated (%): C, 59.72; H, 5.54; B, 11.32; P, 8.11. Found (%): C, 59.48; H, 5.58; B, 11.50; P, 8.32.

3.4. X-ray Diffraction Study of **4a** and **5a**

The X-ray single crystal data were collected using Mo Kα radiation (λ = 0.71073 Å) on Bruker SMART 1000 diffractometer equipped with the Cryostream (Oxford Cryosystems) open-flow nitrogen cryostat. The structures were solved by direct methods and refined by the full-matrix least squares technique against F^2 with anisotropic thermal parameters for all non-hydrogen atoms using the SHELXL software [39]. Hydrogen atoms of the carborane ligands, as well hydride ligand in **5a**, were located from the Fourier syntheses. The remaining hydrogen atoms were placed geometrically and included in the structure factors calculation in the riding motion approximation. Crystal data and parameters of the refinements are listed in Table 2. Crystallographic data for the structures have been deposited with the Cambridge Crystallographic Data Centre as supplementary publications CCDC 2201207–2201208 and can be found in the Supplementary Materials.

Table 2. Crystal data, data collection and structure refinement parameters for **4a** and **5a.**

Compound	4a	5a
CCDC No.	2201207	2201208
Empirical formula	$C_{44}H_{45}B_8ClOP_2Ru_2$	$C_{44}H_{45}B_8ClOP_2Ru \cdots 2(CH_2Cl_2)$
Molecular weight	975.81	1044.59
Temperature (K)	120(2)	110(2)
Crystal system	triclinic	monoclinic
Space group	$P\bar{1}$	$P2_1/c$
a (Å)	10.560(2)	18.467(11)
b (Å)	20.205(4)	15.515(9)
c (Å)	22.352(4)	18.611(11)
α (deg)	114.814(4)	90
β (deg)	101.570(4)	100.170(11)
γ (deg)	90.753(4)	90
V (Å^3)	4215.4(14)	5249(5)
Z	4	4
D_{calc} (g cm^{-3})	1.538	1.322
linear absorption μ (cm^{-1})	8.92	6.47
T_{min}/T_{max}	0.659/0.862	0.560/0.928
$2\theta_{max}$ (deg)	58	52
Reflections collected	54553	45233
Independent reflections (R_{int})	22374 (0.0329)	10275 (0.1263)
Observed reflections ($I > 2\sigma(I)$)	15232	5005
Number of parameters	1102	602
R_1 (on F for $I > 2\sigma(I)$) [a]	0.0462	0.0987
wR_2 (on F^2 for all data) [b]	0.1000	0.2767
GOOF	1.075	1.009
Largest diff. peak/hole (e Å^{-3})	1.792/−0.643	2.931/−1.039

[a] $R_1 = \Sigma\,||F_o| - |F_c||/\Sigma|F_o|$, [b] $wR_2 = \{\Sigma[w(F_o{}^2 - F_c{}^2)^2]/\Sigma w(F_o{}^2)^2\}^{1/2}$.

4. Conclusions

In summary, we showed that the interaction of *arachno*-carborane **3** with ruthenium complex **1** leads to the selective formation of a 10-vertex 20-electron *isocloso*-cluster as the only stable product, whereas an analogous reaction of the phenyl substituted *nido*-carborane **2** produces a complex mixture of cluster compounds. For example, a number of products with the (η^6-Ph)Ru motif were isolated along with other 8- and 10-vertex clusters, and this can be explained by the strong coordination affinity of ruthenium to arene ligands. By contrast, we have shown previously that the related osmium complex $OsCl_2(PPh_3)_3$ provides a more selective polyhedral contraction of monocarbollides [25,26].

Supplementary Materials: The following supporting information can be downloaded at: https://www.mdpi.com/article/10.3390/inorganics10100158/s1, crystallographic data for **4a** and **5a**.

Author Contributions: Conceptualization, V.E.K. and D.A.L.; methodology, D.A.L.; investigation, V.E.K. and M.V.T.; data curation, V.E.K.; X-ray crystallography, F.M.D.; writing—original draft preparation, V.E.K.; writing—review and editing, F.M.D. and D.A.L. All authors have read and agreed to the published version of the manuscript.

Funding: Generous support by the Ministry of Science and Higher Education of the Russian Federation (Contract/agreement No. 075-00697-22-00) is gratefully acknowledged.

Institutional Review Board Statement: Not applicable.

Informed Consent Statement: Not applicable.

Data Availability Statement: Accession codes 2201207 (**4a**) and 2201208 (**5a**) contains the supplementary crystallographic data for this paper. These data can be obtained free of charge via www.ccdc.cam.ac.uk/data_request/cif, or by emailing data_request@ccdc.cam.ac.uk, or by contacting The Cambridge Crystallographic Data Centre, 12 Union Road, Cambridge CB2 1EZ, UK; Fax: +44-1223-336033.

Acknowledgments: We would like to dedicate this work to the memory of Igor T Chizhevsky, who has been the main protagonist of the metallacarborane chemistry in Russia. The single-crystal X-ray diffraction analysis was performed using the equipment of the JRC PMR IGIC RAS.

Conflicts of Interest: The authors declare no conflict of interest.

References

1. Hosmane, N.S. (Ed.) *Boron Science: New Technologies and Applications*; CRC Press: Boca Raton, FL, USA, 2011.
2. Grimes, R.N. *Carboranes*, 3rd ed.; Academic Press: Amsterdam, The Netherlands, 2016.
3. Kar, S.; Pradhan, A.N.; Ghosh, S. *Comprehensive Organometallic Chemistry IV*; Parkin, G., O'Hare, D., Meyer, K., Eds.; Elsevier Science: Amsterdam, The Netherlands, 2022; Volume 9, pp. 263–369.
4. Loginov, D.A.; Konoplev, V.E. Oxidative coupling of benzoic acids with alkynes: Catalyst design and selectivity. *J. Organomet. Chem.* **2018**, *867*, 14–24. [CrossRef]
5. Vinogradov, M.M.; Loginov, D.A. Rhoda- and iridacarborane halide complexes: Synthesis, structure and application in homogeneous catalysis. *J. Organomet. Chem.* **2020**, *910*, 121135. [CrossRef]
6. Molotkov, A.P.; Vinogradov, M.M.; Moskovets, A.P.; Chusova, O.; Timofeev, S.V.; Fastovskiy, V.A.; Nelyubina, Y.V.; Pavlov, A.A.; Chusov, D.A.; Loginov, D.A. Iridium halide complexes [1,1-X_2-8-SMe_2-1,2,8-$IrC_2B_9H_{10}]_2$ (X = Cl, Br, I): Synthesis, reactivity and catalytic activity. *Eur. J. Inorg. Chem.* **2017**, *2017*, 4635–4644. [CrossRef]
7. Grishin, I.D.; Knyazeva, N.A.; Penkal, A.M. Novel ruthenium(II) and (III) carborane complexes with diphosphine ligands and their application in radical polymerization. *Russ. Chem. Bull.* **2020**, *69*, 1520–1529. [CrossRef]
8. Kaltenberg, A.A.; Somov, N.V.; Malysheva, Y.B.; Knyazeva, N.A.; Piskunov, A.V.; Grishin, I.D. Novel carborane complexes of ruthenium with tridentate phosphine ligands: Synthesis and application in atom transfer radical polymerization. *J. Organomet. Chem.* **2020**, *917*, 121291. [CrossRef]
9. Grishin, D.F.; Grishin, I.D. Modern trends in controlled synthesis of functional polymers: Fundamental aspects and practical applications. *Russ. Chem. Rev.* **2021**, *90*, 231–264. [CrossRef]
10. Grishin, I.D.; Zimina, A.M.; Anufriev, S.A.; Knyazeva, N.A.; Piskunov, A.V.; Dolgushin, F.M.; Sivaev, I.B. Synthesis and Catalytic Properties of Novel Ruthenacarboranes Based on *nido*-[5-Me-7,8-$C_2B_9H_{10}]^{2-}$ and nido-[5,6-Me_2-7,8-$C_2B_9H_9]^{2-}$ Dicarbollide Ligands. *Catalysts* **2021**, *11*, 1409. [CrossRef]
11. Loginov, D.A.; Belova, A.O.; Vologzhanina, A.V.; Kudinov, A.R. Cationic iridacarboranes [3-(arene)-3,1,2-$IrC_2B_9H_{11}]^+$ and [3-$(MeCN)_3$-3,1,2-$IrC_2B_9H_{11}]^+$: Synthesis, reactivity, and bonding. Catalysis of oxidative coupling of benzoic acid with alkynes. *J. Organomet. Chem.* **2015**, *793*, 232–240. [CrossRef]
12. Loginov, D.A.; Muratov, D.V.; Nelyubina, Y.V.; Laskova, J.; Kudinov, A.R. μ-Borole triple-decker complexes as catalysts for oxidative couplingof benzoic acid with alkynes. Structure of a hybridrhodacyclopentadienyl/borole triple-decker complex. *J. Mol. Catal. A Chem.* **2017**, *426*, 393–397. [CrossRef]
13. Molotkov, A.P.; Timofeev, S.V.; Loginov, D.A. Trimethylammonium-containing rhodacarborane [(9-NMe_3-7,8-$C_2B_9H_{10}$)$RhCl_2]_2$ as a catalyst for the annulation of arylcarboxylic acids with alkynes. *Russ. Chem. Bull.* **2021**, *70*, 1922–1926. [CrossRef]
14. Kharitonov, V.B.; Muratov, D.V.; Nelyubina, Y.V.; Loginov, D.A. Formation of a Naphthalene Framework by Rhodium(III)-Catalyzed Double C–H Functionalization of Arenes with Alkynes: Impact of a Supporting Ligand and an Acid Additive. *Synthesis* **2022**. [CrossRef]
15. Wang, L.; Perveen, S.; Ouyang, Y.; Zhang, S.; Jiao, J.; He, G.; Nie, Y.; Li, P. Well-Defined, Versatile and Recyclable Half-Sandwich Nickelacarborane Catalyst for Selective Carbene-Transfer Reactions. *Chem. Eur. J.* **2021**, *27*, 5754–5760. [CrossRef] [PubMed]

16. Alekseev, L.S.; Lyubimov, S.E.; Dolgushin, F.M.; Novikov, V.V.; Davankov, V.A.; Chizhevsky, I.T. New Rhodacarborane—Phosphoramidite Catalyst System for Enantioselective Hydrogenation of Functionalized Olefins and Molecular Structure of the Chiral Catalyst Precursor [3,3-{(*S*)-PipPhos}2-3-H-1,2-(*o*-xylylene)-*closo*-3,1,2-$RhC_2B_9H_9$]. *Organometallics* **2011**, *30*, 1942–1950. [CrossRef]
17. Xie, Q.; Wang, T.; Wu, S.; Guo, W.; Zhang, H. A stable ruthenium complex bearing a 1,2-dicarbadodecaborane(12)-1,2-dithiolate ligand and its activation for olefin metathesis. *J. Organomet. Chem.* **2018**, *865*, 95–99. [CrossRef]
18. Chan, A.P.Y.; Parkinson, J.A.; Rosair, G.M.; Welch, A.J. Bis(phosphine)hydridorhodacarborane derivatives of 1,1′-bis(*ortho*-carborane) and their catalysis of alkene isomerization and the hydrosilylation of acetophenone. *Inorg. Chem.* **2020**, *59*, 2011–2023. [CrossRef]
19. Guerrero, I.; Kelemen, Z.; Viñas, C.; Romero, I.; Teixidor, F. Metallacarboranes as Photoredox Catalysts in Water. *Chem. Eur. J.* **2020**, *26*, 5027–5036. [CrossRef]
20. Guerrero, I.; Viñas, C.; Romero, I.; Teixidor, F. A stand-alone cobalt bis(dicarbollide) photoredox catalyst epoxidates alkenes in water at extremely low catalyst load. *Green Chem.* **2021**, *23*, 10123–10131. [CrossRef]
21. Guerrero, I.; Viñas, C.; Fontrodona, X.; Romero, I.; Teixidor, F. Aqueous Persistent Noncovalent Ion-Pair Cooperative Coupling in a Ruthenium Cobaltabis(dicarbollide) System as a Highly Efficient Photoredox Oxidation Catalyst. *Inorg. Chem.* **2021**, *60*, 8898–8907. [CrossRef]
22. Jones, C.J.; Francis, J.N.; Hawthorne, M.F. New 10- and 11-atom polyhedral metallocarboranes prepared by polyhedral contraction. *J. Am. Chem. Soc.* **1972**, *94*, 8391–8399. [CrossRef]
23. Hanusa, T.P.; Huffman, J.C.; Curtis, T.L.; Todd, L.J. Synthesis of (π-arene)metallacarbaboranes containing ruthenium or osmium and a (π-cyclohexadienyl)cobaltacarbaborane. Crystal structure of 2,5,6-(η-C_6H_6)$RuC_2B_7H_{11}$. *Inorg. Chem.* **1985**, *24*, 787–792. [CrossRef]
24. Buckner, S.W.; Fischer, M.J.; Jelliss, P.A.; Luo, R.; Minteer, S.D.; Rath, N.P.; Siemarczuk, A. Dual Fluorescence from an Isonido ReIII Rhenacarborane Phosphine Complex, [7,10-μ-H-7-CO-7,7-$(PPh_3)_2$-*isonido*-7,8,9-$ReC_2B_7H_9$]. *Inorg. Chem.* **2006**, *45*, 7339–7347. [CrossRef] [PubMed]
25. Konoplev, V.E.; Pisareva, I.V.; Vorontsov, E.V.; Dolgushin, F.M.; Franken, A.; Kennedy, J.D.; Chizhevsky, I.T. Ten-vertex osmamonocarbaboranes via *arachno* and *nido* {CB_9} monocarbaboranes. Polyhedral contraction promoted by [$OsCl_2(PPh_3)_3$] in MeOH and the crystal and molecular structure of [1-H-1,1-$(PPh_3)_2$-2-Ph-3-(OMe)-*isocloso*-1,2-$OsCB_8H_7$]. *Inorg. Chem. Commun.* **2003**, *6*, 1454–1458. [CrossRef]
26. Konoplev, V.E.; Dolgushin, F.M.; Loginov, D.A.; Tachaev, M.V. Step-by-step polyhedral contraction of the osmacarborane framework {$OsCB_{10}$} → {$OsCB_9$} → {$OsCB_8$}. *J. Organomet. Chem.* **2021**, *949*, 121948. [CrossRef]
27. Du, S.; Kautz, J.A.; McGrath, T.D.; Stone, F.G.A. Synthesis and Structure of the Novel 11-Vertex Rhenacarborane Dianion [1,1,1-$(CO)_3$-2-Ph-*closo*-1,2-$ReCB_9H_9$]$^{2-}$ and Its Reactivity toward Cationic Transition Metal Fragments. *Organometallics* **2003**, *22*, 2842–2850. [CrossRef]
28. Kolomnikova, G.D.; Petrovskii, P.V.; Sorokin, P.V.; Dolgushin, F.M.; Yanovsky, A.I.; Chizhevsky, I.T. Synthesis, structure and isomerism of "three-bridge" *exo-nido*-osmacarborane clusters. *Rus. Chem. Bull.* **2001**, *50*, 706–715. [CrossRef]
29. Rowland, R.S.; Taylor, R. Intermolecular Nonbonded Contact Distances in Organic Crystal Structures: Comparison with Distances Expected from van der Waals Radii. *J. Phys. Chem.* **1996**, *100*, 7384–7391. [CrossRef]
30. Grimes, R.N.; Sinn, E.; Pipal, J.R. Tetracarbon metallacarboranes. 9. New types of *nido* cage geometry. Crystal and molecular structures of $[(C_6H_5)_2PCH_2]_2Ni(CH_3)_4C_4B_8H_8$ (isomer 1) and (η^5-C_5H_5)$Co(CH_3)_4C_4B_7H_7$ (isomer 2). *Inorg. Chem.* **1980**, *19*, 2087–2095. [CrossRef]
31. Ditzel, E.J.; Fontaine, X.L.R.; Greenwood, N.N.; Kennedy, J.D.; Sisan, Z.; Štíbr, B.; Thornton-Pett, M. An unusual direct conversion of metallaboranes to metallacarbaboranes and the isolation of a novel *isoarachno* twelve-vertex cluster compound. *J. Chem. Soc. Chem. Commun.* **1990**, 1741–1743. [CrossRef]
32. Pisareva, I.V.; Konoplev, V.E.; Petrovskii, P.V.; Vorontsov, E.V.; Dolgushin, F.M.; Yanovsky, A.I.; Chizhevsky, I.T. Synthesis and characterization of novel monocarbollide *exo-closo*-(π-arene)biruthenacarboranes $[(PPh_3)_mClRu(\eta^6\text{-}C_6H_5R)Ru'CB_{10}H_{11\text{-}n}(OMe)_n]$ (where R = H, m = 2, n = 1; R = μ-PPh_2, m = 1, n = 0, 1). *Inorg. Chem.* **2004**, *43*, 6228–6237. [CrossRef]
33. Beckett, M.A.; Brellochs, B.; Chizhevsky, I.T.; Damhus, T.; Hellwich, K.-H.; Kennedy, J.D.; Laitinen, R.; Powella, W.H.; Rabinovich, D.; Viñas, C.; et al. Nomenclature for boranes and related species (IUPAC Recommendations 2019). *Pure Appl. Chem.* **2020**, *92*, 355–381. [CrossRef]
34. Kennedy, J.D. NMR in Inorganic and Organometallic Chemistry. In *Multinuclear NMR*; Mason, J., Ed.; Plenum: London, UK; New York, NY, USA, 1987; p. 221.
35. Chizhevsky, I.T.; Yanovsky, A.I.; Struchkov, Y.T. Semi-sandwich platinum metals metallacarboranes derived from *nido*-$C_2B_9H_{12}^-$: Chemistry and structural studies. *J. Organomet. Chem.* **1997**, *51*, 51–63. [CrossRef]
36. Pisareva, I.V.; Dolgushin, F.M.; Yanovsky, A.I.; Balagurova, E.V.; Petrovskii, P.V.; Chizhevsky, I.T. The first 8-vertex monocarbon metallacarborane with an "isolated" boron-capped pentagonal bipyramidal cage. Synthesis and molecular structure of capped *closo*-2,2-$(Ph_3P)_2$-2-H-3,6,8-$(MeO)_3$-$RuCB_6H_4$. *Inorg.Chem.* **2001**, *40*, 5318–5319. [CrossRef] [PubMed]
37. Perekalin, D.S.; Kudinov, A.R. Cyclopentadienyl ruthenium complexes with naphthalene and other polycyclic aromatic ligands. *Coord. Chem. Rev.* **2014**, *276*, 153–173. [CrossRef]

38. Stephenson, T.A.; Wilkinson, G.J. New complexes of ruthenium (II) and (III) with triphenylphosphine, triphenylarsine, trichlorostannate, pyridine and other ligands. *J. Inorg. Nucl. Chem.* **1966**, *28*, 945–956. [CrossRef]
39. Sheldrick, G.M. Crystal structure refinement with SHELXL. *Acta Crystallogr. C Struct. Chem.* **2015**, *71*, 3–8. [CrossRef]